Modern day Mycobacterium tuberculosis Beijing and East-African Indian strains cause B-cell influx into the lungs compared to an H37Rv-induced T-cell response

Bas C. Mourik[1], Jurriaan E.M. de Steenwinkel[1], Gerjo J. de Knegt[1], Ruth Huizinga[2], Annelies Verbon[3], Tom H.M Ottenhoff[4], Dick van Soolingen[5], Pieter J.M. Leenen[2*]

[1] *Dept. Medical Microbiology & Infectious Diseases, Erasmus MC, Rotterdam, the Netherlands*

[2] *Dept. Immunology, Erasmus University Medical Center, Rotterdam, the Netherlands*

[3] *Dept Internal Medicine, Erasmus University Medical Center, Rotterdam, the Netherlands*

[4] *Dept. of Infectious Diseases, Leiden University Medical Center, Leiden, the Netherlands*

[5] *National Tuberculosis Reference Laboratory, National Institute of Public Health and the Environment (RIVM), Bilthoven, the Netherlands*

ABSTRACT

To identify how virulence among different *Mycobacterium tuberculosis* lineages can influence host responses, we infected BALB/c mice with Beijing-1585, EAI-1627 or the less virulent laboratory strain H37Rv. Disease progression was monitored up to 28 days post infection. Beijing-1585 and EAI-1672 infection resulted in higher mycobacterial loads at earlier time points. They induced a marked influx of B-cells and elevated IL-4 protein levels in the lungs compared to H37Rv, which induced a T-cell influx with higher γγ and IL-17 levels. During infection with Beijing-1585 and EAI-1627, myeloid cells in the lungs appeared functionally impaired with reduced iNOS and IL-12 expression levels compared to H37Rv infection. In the bone marrow of mice infected with Beijing-1585 and EAI-1627 we found reduced expression of IFN-γ, TNF-α and IFN-β, essential for myeloid cell priming, from the third day post infection onwards. Our findings indicate that the increased virulence of two clinical isolates compared to H37Rv is characterized by a fundamentally different systemic immune response, which already can be detected early during infection.

Submitted for publication

INTRODUCTION

Tuberculosis (TB) is a leading cause of death among infectious diseases worldwide and claimed more victims in 2015 than HIV and malaria combined (1). While global efforts have resulted in a steady decline in TB-related deaths over the years, new threats are present in the form of drug resistance and the emergence of more virulent *Mycobacterium tuberculosis* (Mtb) genotypes (1-3).

Mycobacterial strains belonging to the Beijing genotype particularly have shown an aggressive global spread over the last century and have been associated with higher rates of treatment failure and disease relapse compared to other genotypes (4-10). One major explanation for this clinical impact of the Beijing genotypes seems to be their increased capacity to acquire drug resistance (11). A less well-defined characteristic concerns their hypervirulence (12-14). Clinical studies on immunology and pathogenicity of strains belonging to the Beijing genotype are challenging due to varying outcome parameter definitions (15, 16). Nonetheless, Beijing strains cause higher mycobacterial loads, more lung damage and earlier mortality compared to strains from other lineages in preclinical TB models (13, 17, 18). Mechanistic studies have suggested that Beijing strains have enhanced capacity to inhibit protective immunity in the lungs through induction of higher levels of type-I interferons, leading to lower IL-12 and TNF-α levels and reduced T-cell activation (19, 20). Increased Beijing virulence also has been attributed to bacterial phenolic glycolipid (PGL)-production, which suppresses the production of IL-12, IL-6 and TNF-α by host immune cells (21, 22). Lastly, Beijing strains may induce a stronger regulatory T-cell response compared to other strains, thereby down-regulating protective immunity (17, 23).

One factor hampering Beijing genotype-specific immunological characterization is the genetic diversity among Beijing strains, which can substantially affect virulence (3, 24). In this study we evaluate the host response during acute infection against the well-defined, highly virulent Beijing-1585 strain. This strain has previously demonstrated similar infection and mortality kinetics as other virulent Beijing strains (18, 24). Furthermore, Beijing-1585 was found associated with drug resistance and treatment failure (18, 25). We compare Beijing-1585 with a clinical isolate from the East-African/Indian (EAI) lineage that displays similar virulence as Beijing-1585 in our model (18), and with the less virulent laboratory strain H37Rv (26).

Previous studies in our (BALB/c) mouse TB model showed that mice infected with the laboratory strain H37Rv reach maximal mycobacterial loads and start developing progressive pneumonia 28 days post infection (dpi). Next, they enter a phase of chronic

infection and become moribund between 22 and 38 weeks post infection (26). In contrast, mice infected with Beijing-1585 or EAI-1627 reach peak infection at 14 dpi with histopathological signs of pneumonia comparable to H37Rv at 28 dpi and rapidly become moribund between three to five weeks post infection if left untreated (26, 27). In this study we aim to identify the underlying host responses that might contribute to this marked difference in virulence.

MATERIALS AND METHODS

Mycobacterial strains

We used the *Mycobacterium tuberculosis* H37Rv strain (ATCC 27294) and two strains isolated from patients in Vietnam in 2002, Beijing-1585 and EAI-1627, as representatives for their respective lineage based on genotyping results (27).

Mice and infection

Female specific pathogen-free BALB/c mice aged 10-11 weeks and weighing 22-24 grams (Charles River, Les Oncins, France) were infected by intra-tracheal instillation under general anesthesia as described previously (25). Inoculum sizes were confirmed by plating and were $1.0.10^5$ colony forming units (CFU) for Beijing-1585, $1.3.10^5$ CFU for EAI-1627 and $1.8.10^5$ CFU for H37Rv. Mice infected with Beijing-1585 or EAI-1627 rapidly become moribund between 3-5 weeks (18), therefore mycobacterial loads and other parameters for these two clinical strains were measured up to the peak of infection at 14 dpi, while measurements on H37Rv-infected animals were continued up to peak of infection at 28 dpi. All protocols were approved by the institutional animal ethics committee (DEC number 117-12-13, EMC-number 3005) and adhered to the rules laid down in the Dutch Animal Experimentation Act and the EU Animal Directive 201/63/EU.

Determination of mycobacterial load

Lungs and spleens were removed aseptically and homogenized in 2 mL PBS using the gentleMACS Octo Dissociator (Miltenyi Biotec BV, Leiden, the Netherlands) according to the manufacturer's protocol. From each tissue homogenate 10-fold serial dilutions were made. Next, 200 µL aliquots were plated on 7H10 agar culture plates supplemented with 10% OADC. Plates were incubated for up to 42 days at 37 °C and 5% CO_2 before colonies were counted.

Flow cytometry, Real-time quantitative PCR and Cytokine assessment

The flow cytometry protocol, fluorescent antibody panels, Real-time quantitative PCR and Cytokine assessment were essentially as described previously (29). An additional

fluorescent antibody panel used in this study is described in **supplementary Table 1**. Primer sequences and manufacturers are listed in **supplementary Table 2**.

Data analysis and statistics

Flow cytometry data were analyzed using Flowjo 7.6.5. Analyses were done and graphs were made using PRISM Graphpad 7. All data are expressed as mean ± SEM. Student's t-test, followed by Bonferroni correction for multiple comparisons where applicable, was used to calculate significance, except for **Fig**. **7B**. Here we used two-way, repeated measure ANOVA. P-values less than 0.05 were considered statistically significant.

RESULTS

Beijing-1585 and EAI-1627 lead to higher mycobacterial loads than H37Rv at earlier time points

We found no significant differences in mycobacterial load between Beijing-1585, EAI-1627 and H37Rv at 1 dpi and 3 dpi, indicating that all groups received a similar inoculum of mycobacteria (**Fig. 1A**). At 7 dpi, mice infected with Beijing-1585 had significantly higher mycobacterial loads than mice infected with EAI-1627 or H37Rv and at 14 dpi, Beijing-1585 and EAI-1627 caused almost 2 log higher loads than H37Rv. Mycobacterial loads for H37Rv at peak infection (28 dpi) were still 1 log lower than those observed for Beijing-1585 and EAI-1627 at 14 dpi. These findings are in agreement with previous studies monitoring mycobacterial loads for Beijing strains and H37Rv (13, 28).

To check whether the higher mycobacterial loads in the lungs caused by Beijing-1585 and EAI-1627 were associated with more rapid dissemination to other organs, we determined mycobacterial loads in the spleen (**Fig. 1B**). No significant differences in culture-conversion were found. At 7 dpi the Beijing-1585 group did show culture-positive spleens in all mice with higher loads compared to other groups.

Beijing-1585 and EAI-1627 induce lung influx of B-cells, while H37Rv induces T-cell influx

To explore whether the distinct mycobacterial growth profiles in our model correlated with differences in adaptive immune responses, we evaluated the numbers of B- and T-cells recruited to the lungs by the three different strains. Most notably, Beijing-1585 and EAI-1627 induced a strong influx of B-cells at 14 dpi, which was not observed for H37Rv at either 14 dpi or 28 dpi (**Fig. 2A**). In contrast, H37Rv induced the recruitment of $CD4^+$ and $CD8^+$ T-cells at 28 dpi, which was not observed upon infection with the clinical strains (**Fig. 2B/C**). Despite the marked T-cell increase in the H37Rv group at 28

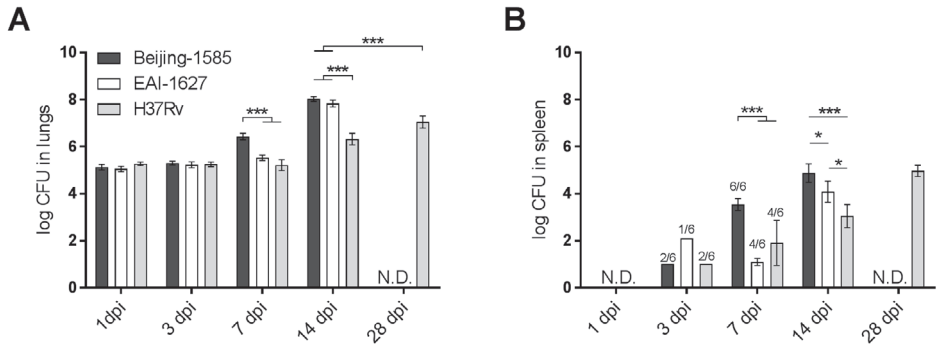

Figure 1. Mycobacterial loads in lungs and spleen

A) Mycobacterial loads in the lungs after intratracheal infection with Beijing-1585 (black bars), EAI-1627 (open bars) or H37Rv (grey bars). At 14 dpi, Beijing-1585 and EAI-1627 cause higher loads than H37Rv at either 14 dpi or 28 dpi (peak infection H37Rv). After 14 days Beijing-1585 and EAI-1627-infected mice rapidly become moribund, therefore no later analyses for these strains are possible. **B)** Mycobacterial loads in the spleen. Dissemination rates from the lungs to the spleens are not significantly different. Beijing-1585-infected mice showed higher loads at 7 dpi and 14 dpi compared to the other strains. Three mice were used for each group at 1 dpi and 6 mice for each group at the remaining time points. Inoculum sizes were $1.0.10^5$ CFU for Beijing, $1.3.10^5$ CFU for EAI and $1.8.10^5$ CFU for H37Rv. * $p < 0.05$ ** $p < 0.01$ *** $p<0.001$ after Bonferroni correction.

dpi, Foxp3$^+$ regulatory T-cells percentages of total lung single cell suspension remained lower compared to Beijing-1585 and EAI-1627 at 14 dpi (**Fig. 2D**). The total lung single cell suspension included parenchymal cells, which function as an internal control as it is reasonable to assume that their numbers remain constant during infection.

Figure 3 shows the associated cytokine protein levels in the lungs for each time point and genotype strain. In accordance with the increase in B-cells, Beijing-1585 and EAI-1627-infected mice showed elevated protein levels of IL-4 at 14 dpi, which were 4-5 fold higher than IL-4 levels observed for H37Rv at 14 and 28 dpi (**Fig. 3A**). Although Beijing-1585 and EAI-1627 also caused elevated protein levels of IFN-γ and IL-17a at 14 dpi, these remained 2-fold and 6-fold lower respectively, compared to the H37Rv group at 28 dpi (**Fig. 3B/C**).

TNF-α protein levels in the lungs closely correlated with strain-dependent differences in mycobacterial loads over time. At 7 dpi, TNF-α levels were significantly induced only in mice infected with Beijing-1585- and EAI-1627, which were almost 2-fold higher at 14 dpi compared to H37Rv at 28 dpi (**Fig. 3D**). This is in line with the role of TNF-α as general inflammation marker. In support of this, the inflammation marker IL-6 showed similar kinetics as TNF-α over time (**Fig S1**). IL-10 and IL-23 levels were also measured in the lung homogenates, but were below the limit of detection of our assay (data not

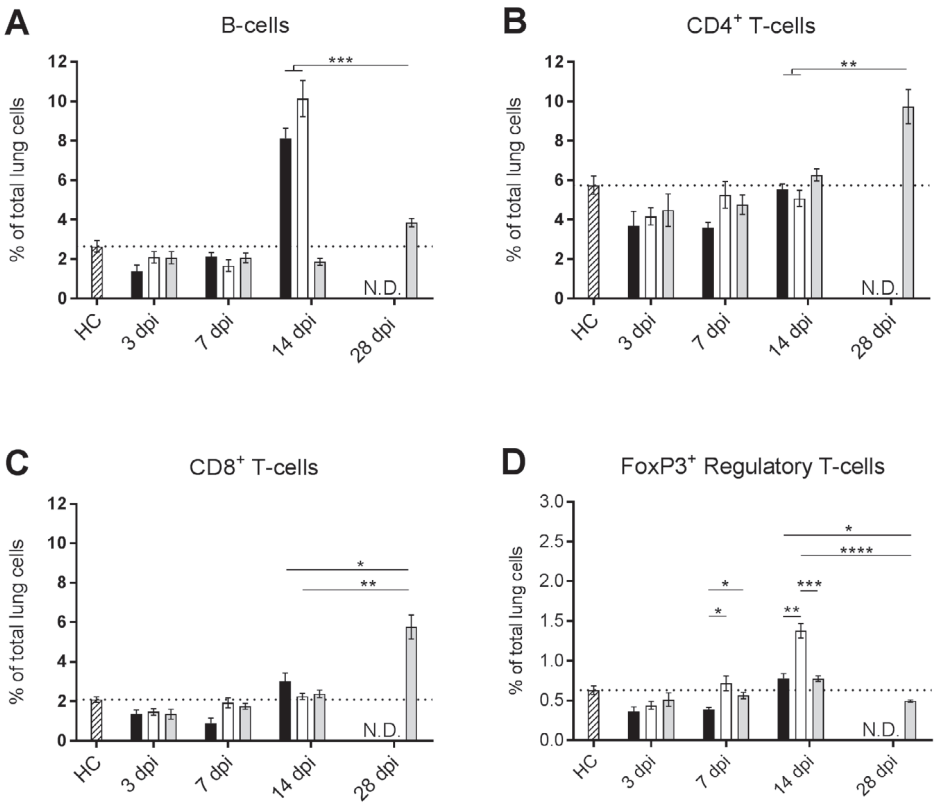

Figure 2. Lymphoid cell populations in the lungs of mice infected with different Mtb strains
Lymphoid cells were determined in the lungs of mice infected with Beijing-1585 (black bars), EAI-1627 (open bars) or H37Rv (grey bars) and compared to healthy control mice (HC, striped bars). **A)** B-cells are significantly higher for Beijing-1585 and EAI-1627 at 14 dpi compared with H37Rv at 14 and 28 dpi. **B/C**) Only H37Rv shows an increase in both $CD4^+$ and $CD8^+$ T-cells at 28 dpi. **D**) Despite the increase in T-cells caused by H37Rv infection at 28 dpi, $Foxp3^+$ regulatory T-cells are significantly lower compared to Beijing-1585- and EAI-1627-infected mice at 14 dpi. Gating strategies were similar as described previously (29). N=6 mice per group per time point, * $p < 0.05$, ** $p < 0.01$, *** $p < 0.001$ after Bonferroni correction. Data are shown as % of total lung single cell suspension including parenchymal cells. These cells function as an internal control as it is reasonable to assume that their numbers remain constant during infection.

shown). Quantitative PCR measurements of IFN-γ, IL-17a TNF-α, IL-6 in the lungs were also performed with outcomes comparable to those on protein level as shown in **Figure 3** (**Fig. S2**). IL-10 expression levels were above the lower limit of detection, but did not show strain-specific differences (**Fig. S2**).

Beijing-1585 and EAI-1627 induce a qualitatively impaired myeloid response compared to H37Rv.

Next, we evaluated potential differences in $CD11b^+$ myeloid cells in the lungs that could explain the observed differences in lymphoid cell responses and cytokine levels. Lung polymorphonuclear leukocytes (PMN) percentages were increased in the Beijing-1585 and EAI-1627 group compared to H37Rv at 7 dpi and 14 dpi, which was in line with the elevated mycobacterial loads and inflammation markers TNF-α and IL-6 at these time points (**Fig. 4A**). However, at 28 dpi the PMN frequency in the H37Rv group was comparable with that in the Beijing-1585 group and EAI-1627 group at 14 dpi.

Inflammatory macrophages / dendritic cells (iM/DC) showed a similar trend as PMN (**Fig. 4B**). Monocyte-like cells were present to a lesser extent than PMN and iM/DC, and were only higher in the EAI-1627 group at 14 dpi compared to the H37Rv group at 28 dpi (**Fig. 4C**). Alveolar macrophages (AM) were reduced over time in all groups, associated with inflammatory cell influx, but most prominently at 14 dpi in the Beijing-1585 and EAI-1627 groups compared to the H37Rv group (**Fig. 4D**). We also evaluated lung eosinophils in each group since these cells are known IL-4 producers, but levels of these cells were not elevated in the Beijing-1585 and EAI-1627 groups compared to the H37Rv group at any time point evaluated (**Fig. S3**).

AM and iM/DC are important cellular sources of IL-12 in the lungs (30), which is essential for initiation of T-cell responses (31). To determine potential functional differences between the infiltrating iM/DC and the lung-resident AM in the different groups, we measured the expression of IL-12p35 and IL-12p40. Most notably, Beijing-1585 caused the strongest down-regulation of IL-12p35 in the lungs compared to healthy control mice and did not induce any IL-12p40 expression at all time points evaluated (**Fig 5A and 5B**).

We also measured the expression of inducible nitric oxide synthase (iNOS) in both cell populations at each time point evaluated. iNOS expression is induced by IFN-γ and TNF-α and associates with bactericidal activity (30, 32). The AM from mice infected with Beijing-1585 failed to up-regulate iNOS at any point during the course of infection (**Fig. 5C**). In contrast, iNOS expression was already significantly higher in AM from H37Rv-infected mice at 3 dpi and its expression continued to increase up to 14 dpi. The expression of iNOS could not be determined in AM of H37Rv-infected mice at 28 dpi as the AM-population at this point was too small to be clearly separated from other cell populations (**Fig 4D/ Fig S4A**).

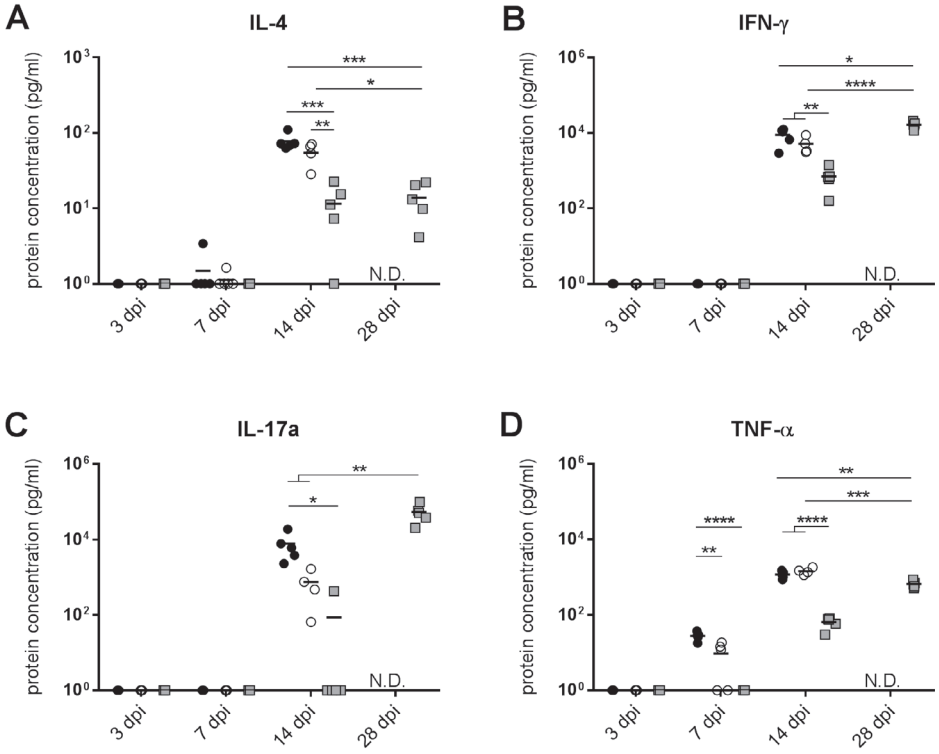

Figure 3. Cytokine protein levels in the lungs of mice infected with different Mtb strains
Protein levels were determined in lung tissue homogenates of mice infected with Beijing-1585 (black dots), EAI-1627 (open circles) or H37Rv (grey squares). **A)** IL-4 levels are 4-5 fold higher for Beijing-1585 and EAI-1627 at 14 dpi compared to H37Rv at 14 dpi or 28 dpi. **B)** IFN-γ levels are elevated for Beijing-1585 and EAI-1627 at 14 dpi, but are 2-fold lower compared to H37Rv at 28 dpi. **C)** Beijing-1585 and EAI-1627 induced circa 7-fold lower levels of IL-17a at 14 dpi compared to H37Rv at 28 dpi. **D)** TNF-α levels are circa 2-fold higher for Beijing-1585 and EAI-1627 at 14 dpi compared to H37Rv at 28 dpi. N=6 mice per group per time point, * $p < 0.05$, ** $p < 0.01$, *** $p < 0.001$, **** $p < 0.0001$ after Bonferroni correction.

iM/DC in lungs of mice infected with Beijing-1585 or EAI-1627 also showed significantly lower iNOS expression compared to H37Rv-infected mice at 3 dpi and 7 dpi (**Fig 5D**). At 14 dpi, when IFN-γ and TNF-α levels were high in the lungs of mice from the Beijing-1585 and EAI-1627 group (**Fig. 3C**), iNOS expression by iM/DC was increased accordingly. Nevertheless, iNOS expression by iM/DC in H37Rv-infected mice was significantly higher at 14 dpi despite lower levels of IFN-γ and TNF-α in the lungs compared to Beijing-1585- and EAI-1627-infected mice and iNOS expression levels increased even further at 28 dpi.

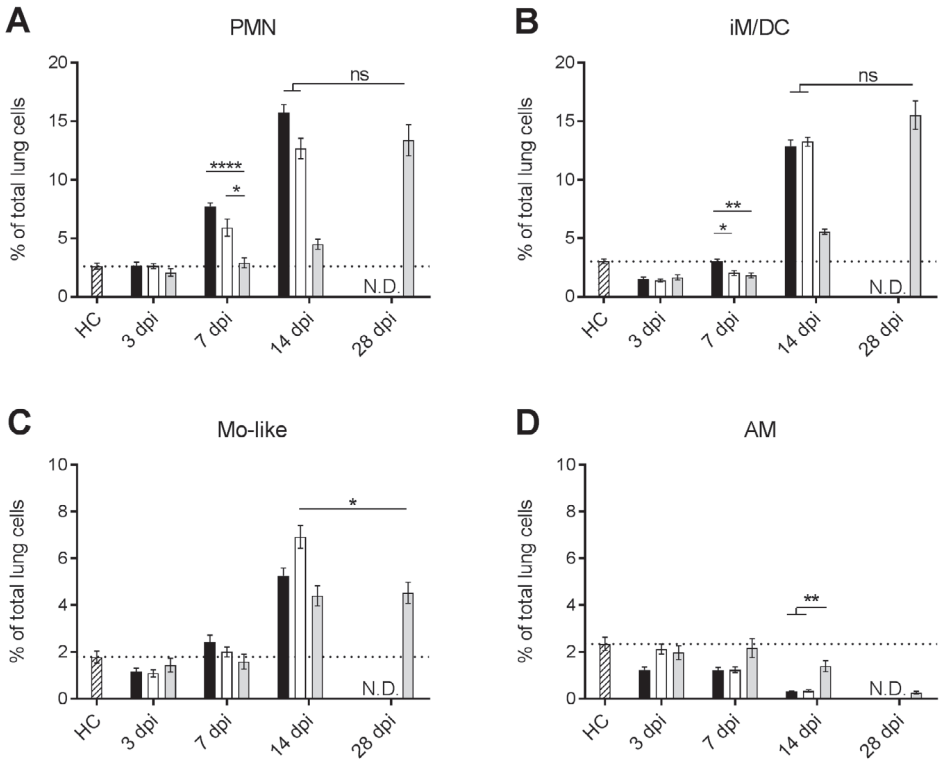

Figure 4. Myeloid cell populations in the lungs of mice infected with different Mtb strains
CD11b^{+} cells were distinguished as PMN, iM/DC, monocyte-like cells (Mo-like) and AM in the lungs of mice infected with Beijing-1585 (black bars), EAI-1627 (open bars) or H37Rv (grey bars) compared to healthy control mice (HC, striped bars). **A)** PMN (CD11b^{+}Ly6G^{high}) cells showed a more rapid increase for Beijng-1585 and EAI-1627 compared to H37Rv. **B)** iM/DC (CD11b^{+}Ly6C^{int}CD11c^{high}) showed kinetics comparable to PMN for the different groups. **C)** Monocyte-like cells (CD11b^{+}Ly6C^{high}CD11c^{low}) are only higher in the EAI-1627 group at 14 dpi compared to the H37Rv group at 28 dpi. **D)** Lung alveolar macrophages (CD11b^{int}CD11c^{high}SiglecF^{+}) are lower in the Beijing-1585 and EAI-1627 group compared to the H37Rv group at 14 dpi. N=6 mice per group per time point, * $p < 0.05$, ** $p < 0.01$, *** $p < 0.001$ after Bonferroni correction.

Infection with Beijing-1585 induces less expression of inflammatory cytokines in the bone marrow compared to H37Rv

To assess if iM/DC from the H37Rv-infected group were primed differently at an earlier developmental stage, we determined cytokine mRNA expression in the bone marrow in the course of infection.

Similar to the lungs, IL-12p35 mRNA expression in the bone marrow was down-regulated most effectively by Beijing-1585 infection compared to uninfected mice at all time points evaluated (**Fig. 6A**). Interestingly, Beijing-1585 infection also showed a lack of induction, or even reduced expression of inflammatory cytokines IFN-γ, IL-17a and

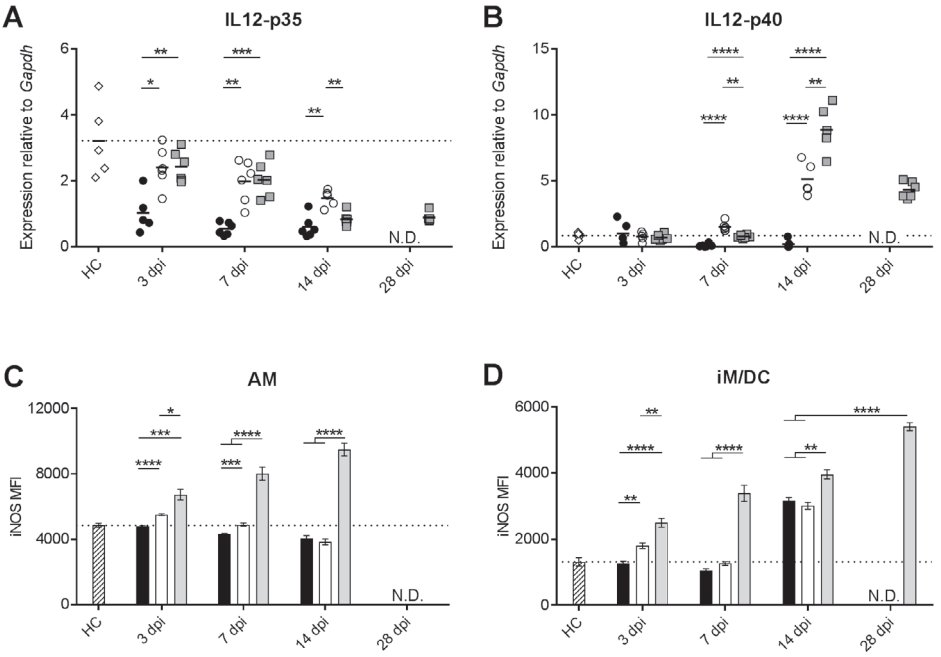

Figure 5. IL-12 production and myeloid cell populations iNOS expression in the lungs of Mtb-infected mice

IL-12 mRNA expression in total lung homogenate (**A,B**) and iNOS expression in alveolar macrophages (AM) and inflammatory macrophages/dendritic cells (iM/DC) in the lungs (**C,D**) of mice infected with Beijing-1585 (black bars/dots), EAI-1627 (open bars/dots) or H37Rv (grey bars/squares) are compared to healthy control mice (HC, striped bars/open diamonds). **A)** IL-12p35 expression levels are lower in the Beijing-1585 group compared to the EAI-1627 and H37Rv group. **B)** IL-12p40 expression is induced in EAI-1627- and H37Rv-infected mice, and reached its peak for both strains at 14 dpi with higher expression in the H37Rv group. Beijing-1585 does not induce any notable expression of either IL-12p35 or IL-12p40 at all time points evaluated. **C**) AM in the lungs of Beijing-1585-infected mice fail to induce iNOS expression beyond levels observed in healthy control mice. **D)** iM/DC in H37Rv-infected mice show higher iNOS expression than iM/DC in the lungs of mice from the Beijing-1585 or EAI-1627 group at all time point evaluated. N=6 mice per group per time point, * $p < 0.05$, ** $p < 0.01$, *** $p < 0.001$ after Bonferroni correction. For experiments depicted in this figure, iM/DC are defined as $CD11b^{high}CD11c^{high}MHC\text{-}II^{+}$ cells and AM were defined as $CD11b^{int}CD11c^{+}F4/80^{+}CD200R^{+}$ cells (gating strategies: **Fig. S4A**), based on a distinct panel of antibodies. Population frequencies through this gating were highly comparable to those in **Figure 4** (**Fig. S4B**).

TNF-α compared to H37Rv as early as 3 dpi (**Fig. 6B-D**). Especially for TNF-a, expression levels differed markedly between BM cells from Beijing-1585- and H37Rv-infected mice over time with a decreased expression for Beijing-1585 at 14 dpi compared to 3 dpi, as opposed to a 34-fold increase for H37Rv. Measurement results for the EAI-1627 group consistently were intermediate between those for the Beijing-1585 and H37Rv groups, but tended to be more similar to results from Beijing-infected mice.

Induction of type 1 IFN signature genes in the lungs of infected mice essentially correlates with expression of IFN-β

Lastly, we tested the mRNA expression of IFN-α genes (subtypes 1,2,5,6 and 7) in the lungs with methods described by Manca et al (20). We only found a limited expression of the tested IFN-α genes at 3 dpi for all strains, which decreased upon progressing infection and showed no significant inter-strain differences (**Fig. 7A**).

Since IFN-α and IFN-β share the ability to bind to, and signal via the IFN-α/β receptor, we evaluated IFN-β mRNA expression in the lungs. IFN-β expression in the H37Rv group was significantly higher than that in the EAI-1627 group at 3 dpi, and also higher than that in the Beijing-1585 group, but without statistical significance (**Fig. 7B**).

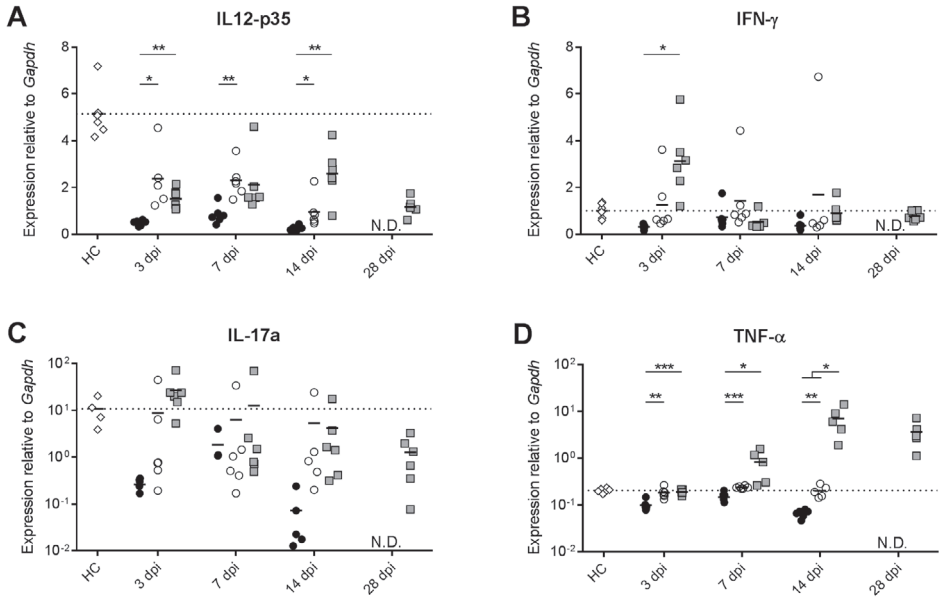

Figure 6. Cytokine mRNA expression levels in the bone marrow of mice infected with different Mtb strains.

Expression levels of target cytokine mRNA are shown relative to *Gapdh* in the bone marrow of mice infected with Beijing-1585 (black dots), EAI-1627 (open circles) or H37Rv (grey squares). **A)** IL-12p35 expression at 3 dpi and 7 dpi was lower in the Beijing-1585 group compared to H37Rv. **B)** IFN-γ expression was lower for Beijing-1585 at 3 dpi compared to H37Rv. **C)** IL-17a levels were markedly lower in the Beijing-1585 group compared to the H37Rv group (mean of 0.26 vs. 26.7), but without statistical significance (p= 0.06 after Bonferroni correction) due to the high spread in the H37Rv group (5.3 – 71.8). **D)** TNF-α levels were higher in the bone marrow of H37Rv-infected mice compared to Beijing-1585-infected mice at all time points evaluated. EAI-1585 consistently showed intermediate results between Beijing-1585 and H37Rv for all cytokines. N=6 mice per group per time point, * $p < 0.05$, ** $p < 0.01$, *** $p < 0.001$, **** $p < 0.0001$ after Bonferroni correction.

Type I interferons comprise several more subtypes than those for which we could test expression by qPCR and their expression is often transient. Therefore we decided to test the type 1 interferon response, represented by expression of *Mx1*, *IFI44* and *CCL2*, which are known type 1 interferon-inducible genes (33-35). Expression levels of such genes can be combined into a type 1 interferon signature, which provides an indication of type 1 interferon responsiveness in a tissue (36). Our type 1 interferon signature showed different kinetics between Beijing-1585 and H37Rv, with EAI-1627 again showing intermediate results (**Figure 7C,** see **Fig S5** for individual graphs). Most notably, the Beijing-1585 group showed the strongest induction of type 1 interferon inducible

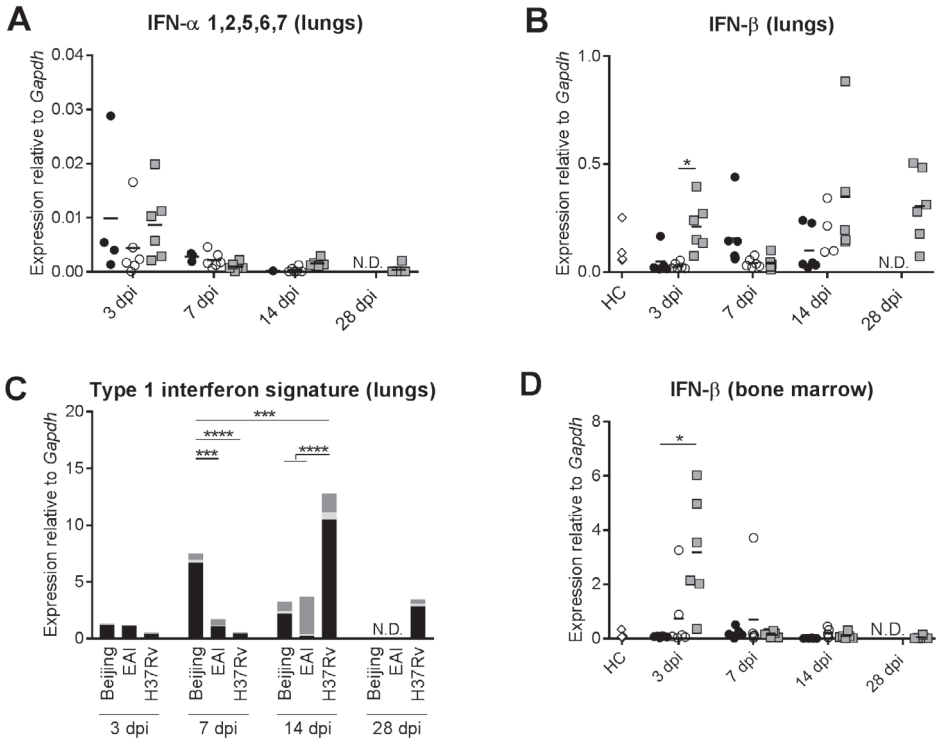

Figure 7. Expression of IFN-α, IFN-β and type 1 interferon-inducible genes in lung and BM during infection with different Mtb strains.

A) Combined expression of IFN-α 1,2,5,6,7 mRNA in lung homogenate did not show significant differences between groups **B)** Expression of IFN-β mRNA in lung homogenate is higher in the lungs of H37Rv-infected mice compared to EAI-1627-infected mice at 3 dpi. Other differences did not reach significance. **C)** Combined expression in the lungs of type 1 interferon-inducible genes *Mx1* (black), *IFI44* (light grey) and *CCL2* (dark grey), represented in a type 1 interferon signature, showed the highest level in the Beijing-1585 group at 7 dpi and in the H37Rv group at 14 dpi. **D)** Expression of IFN-β in the bone marrow is higher in the H37Rv group compared to Beijing-1585 at 3 dpi. N=6 mice per group per time point, * $p < 0.05$, ** $p < 0.01$, *** $p < 0.001$ after Bonferroni correction. Two-way, repeated measure ANOVA followed by Bonferroni correction was used to calculate significance for Figure 7C.

genes in the lungs at 7 dpi, while H37Rv-infected mice showed a higher peak induction at 14 dpi. The observed kinetics for the type 1 interferon-inducible genes at 7 dpi and 14 dpi closely matched the trends observed for IFN-β expression at these time points, and not IFN-α, except for the absence of a type 1 interferon signature in the lungs of mice infected with H37Rv 4 days before. This suggests that in this model IFN-β is more relevant for the induction of type 1 IFN-regulated genes during acute infection than the tested IFN-α subtypes.

To compare the findings on IFN-β in the lungs at 3 dpi with differential systemic effects observed previously in the bone marrow, we measured IFN-β mRNA expression in the bone marrow. This showed a significantly increased expression of IFN-β in the H37Rv group compared to the Beijing-1585 group at 3 dpi (**Fig. 7D**).

DISCUSSION

This study shows that infections with two clinical isolates of *Mycobacterium tuberculosis* belonging to the Beijing and EAI lineages is characterized in the lungs by an influx of B-cells, higher IL-4 protein levels and recruitment of myeloid cells that appear functionally impaired with low IL-12 and iNOS expression levels. Moreover, especially Beijing-1585 infection is associated with a reduced expression of inflammatory cytokines in the bone marrow as early as from 3 dpi onwards, suggesting the hampered priming of developing myeloid cells for subsequent responses.

Our model suggests a pathogenic effect of B-cells during acute infection, thereby contrasting an earlier study that showed that B-cells reduced neutrophilia by limiting IL-17 responses (37). We found lower IL-17 protein levels in the lungs of Beijing-1585- and EAI-1627-infected mice compared to H37Rv and a similar influx of PMN into the lungs at peak infection. These findings were in line with more recent studies demonstrating a protective effect of IL-17 during acute infection, particularly against Beijing strains (38, 39). Another study in non-human primates showed that B-cell depletion resulted in lower levels of inflammation and increased bacterial burdens during acute infection (40). Similarly, we found that the higher percentages of B-cells were associated with higher levels of inflammation, as expressed by inflammation markers TNF-α and IL-6, but also with higher bacterial burdens. Potential interactions between B-cells, IL-17 and inflammation during acute TB are complex and reviewed elsewhere (41). However, based on our data it appears that the combination of a B-cell influx and high IL-17 protein levels in the lungs during acute infection causes excessive inflammatory damage without having

an effective bactericidal effect. Interestingly, during chronic infection a protective role was recently demonstrated for B-cells and antibodies in TB patients (42, 43).

Beijing-1585 and EAI-1627 infection elicited significant IL-4 protein levels in the lungs, thus matching the observed increase in B-cells. The presence of IL-4 was previously shown to exert a pathogenic effect during Mtb infection by diverting the role of TNF-α from myeloid cell activator to tissue damage mediator (44). In line with this, *in vitro* studies showed that Beijing-HN878, another highly virulent Beijing strain, preferentially induced IL-4 expression in human peripheral blood mononuclear cells compared to the CDC1551 strain (45), and that virulent Beijing strains induced higher IL-4 mRNA expression levels in the lungs of mice at 14 dpi compared to non-virulent Beijing strains (24). This adds to the support for a negative role of IL-4 and B-cell responses during acute infection.

The lack of T-cell influx into the lungs observed for Beijing-1585 and EAI-1627 compared to H37Rv can potentially be explained by differences found in IL-12 expression, which is essential for dendritic cell migration from the lungs to the lymph node and the initiation of T-cell responses (31, 46). Our findings that Beijing-1585 induced lower lung IL-12p35 and IL-12p40 mRNA expression levels compared to H37Rv, are in line with previous studies (20, 21, 45, 47). Also the observed lower iNOS-expression levels in AM and iM/DC of mice infected with Beijing-1585 compared to H37Rv were described previously (13, 24, 48). However, these earlier studies found that low iNOS expression was accompanied by low expression levels of iNOS-inducing IFN-γ and TNF-α mRNA (32). In sharp contrast, we observed lower iNOS expression by iM/DC in the lungs at 14 dpi in Beijing-1585- and EAI-1627-infected mice accompanied with significantly higher lung protein levels IFN-γ and TNF-α compared to H37Rv.

Low iNOS expression in AM and iM/DC in the lungs despite high IFN-γ protein levels could be due to inhibition or prevention of iNOS induction at the site of infection. Alternatively, these myeloid cells recruited to the lung might have been primed differently in an earlier stage of development. Gut mucosal immunology studies have shown how local IL-12 production can exert a systemic effect by stimulating bone marrow resident NK-cells to produce IFN-γ early during infection, thereby priming immature myeloid cells to inhibit pathological inflammatory responses in the periphery (49). We have previously reasoned that a similar mechanism might be present in TB (41). In the current study we provide experimental evidence that reduced IL-12 expression in the lungs of Beijing-1585-infected mice is associated in the bone marrow with reduced IL-12 and IFN-γ, as well as reduced IL-17a and TNF-α expression. This occurs already in the early stage of infection before widespread bacterial dissemination. While not conclusive, this

suggests that IL-12-mediated differential bone marrow priming of myeloid cells might be an important factor early during infection with *Mycobacterium tuberculosis*. In this case, lung IL-12 present for H37Rv, but absent for the clinical strains, could cause IFN-γ mediated myeloid cell development in the bone marrow towards a regulatory phenotype that prevents excessive innate inflammatory damage upon their migration to the lungs, while concomitantly stimulating protective adaptive responses.

Next to differential expression of IFN-γ in the bone marrow, we also found significant differences in type 1 interferon expression and responses in both bone marrow and lung. Manca *et al*. have associated virulent Beijing-HN878 infection with elevated IFN-α mRNA expression in the lungs at 28 dpi in a low-dose BALB/c infection model (19, 20). We were unable to reproduce this preferential increase in IFN-α mRNA upon infection with the virulent Beijing strain in the lungs, which could be due to using a high-dose infection model and/or measurements at different time points. In our subsequent analysis of IFN-β expression and type 1 interferon-inducible genes we found lower expression levels for Beijing-1585 and EAI-1627 compared to H37Rv, thus refuting the association of type 1 interferon activity and Mtb virulence in our model.

ACKNOWLEDGMENTS

The authors thank S. van den Berg and M. T. ten Kate from the Department of Medical Microbiology and Infectious Diseases, M. A. W. Smits, A. van Oudenaren and L. Hogenkamp from the Department of Immunology for their technical support, and J. Hagoort from the Department of Communication for his critical reading of the manuscript. Research for this manuscript was (in part) performed within the framework of the Erasmus post-graduate school Molecular Medicine.

REFERENCES

1. WHO Global tuberculosis report 2017.
2. Manson AL, Cohen KA, Abeel T, Desjardins CA, Armstrong DT, Barry CE, 3rd, et al. Genomic analysis of globally diverse Mycobacterium tuberculosis strains provides insights into the emergence and spread of multidrug resistance. Nat Genet. 2017;49(3):395-402.
3. Merker M, Blin C, Mona S, Duforet-Frebourg N, Lecher S, Willery E, et al. Evolutionary history and global spread of the Mycobacterium tuberculosis Beijing lineage. Nat Genet. 2015;47(3):242-9.
4. Sun YJ, Lee AS, Wong SY, Paton NI. Association of Mycobacterium tuberculosis Beijing genotype with tuberculosis relapse in Singapore. Epidemiol Infect. 2006;134(2):329-32.
5. Huyen MN, Buu TN, Tiemersma E, Lan NT, Dung NH, Kremer K, et al. Tuberculosis relapse in Vietnam is significantly associated with Mycobacterium tuberculosis Beijing genotype infections. J Infect Dis. 2013;207(10):1516-24.
6. Parwati I, Alisjahbana B, Apriani L, Soetikno RD, Ottenhoff TH, van der Zanden AG, et al. Mycobacterium tuberculosis Beijing genotype is an independent risk factor for tuberculosis treatment failure in Indonesia. J Infect Dis. 2010;201(4):553-7.
7. Gurjav U, Erkhembayar B, Burneebaatar B, Narmandakh E, Tumenbayar O, Hill-Cawthorne GA, et al. Transmission of multi-drug resistant tuberculosis in Mongolia is driven by Beijing strains of Mycobacterium tuberculosis resistant to all first-line drugs. Tuberculosis (Edinb). 2016;101:49-53.
8. Hang NT, Maeda S, Keicho N, Thuong PH, Endo H. Sublineages of Mycobacterium tuberculosis Beijing genotype strains and unfavorable outcomes of anti-tuberculosis treatment. Tuberculosis (Edinb). 2015;95(3):336-42.
9. Burman WJ, Bliven EE, Cowan L, Bozeman L, Nahid P, Diem L, et al. Relapse associated with active disease caused by Beijing strain of Mycobacterium tuberculosis. Emerg Infect Dis. 2009;15(7):1061-7.
10. Casali N, Nikolayevskyy V, Balabanova Y, Harris SR, Ignatyeva O, Kontsevaya I, et al. Evolution and transmission of drug-resistant tuberculosis in a Russian population. Nat Genet. 2014;46(3):279-86.
11. Parwati I, van Crevel R, van Soolingen D. Possible underlying mechanisms for successful emergence of the Mycobacterium tuberculosis Beijing genotype strains. Lancet Infect Dis. 2010;10(2):103-11.
12. Domenech P, Zou J, Averback A, Syed N, Curtis D, Donato S, et al. Unique Regulation of the DosR Regulon in the Beijing Lineage of Mycobacterium tuberculosis. J Bacteriol. 2017;199(2).
13. Lopez B, Aguilar D, Orozco H, Burger M, Espitia C, Ritacco V, et al. A marked difference in pathogenesis and immune response induced by different Mycobacterium tuberculosis genotypes. Clin Exp Immunol. 2003;133(1):30-7.
14. van Laarhoven A, Mandemakers JJ, Kleinnijenhuis J, Enaimi M, Lachmandas E, Joosten LA, et al. Low induction of proinflammatory cytokines parallels evolutionary success of modern strains within the Mycobacterium tuberculosis Beijing genotype. Infect Immun. 2013;81(10):3750-6.
15. Drobniewski F, Balabanova Y, Nikolayevsky V, Ruddy M, Kuznetzov S, Zakharova S, et al. Drug-resistant tuberculosis, clinical virulence, and the dominance of the Beijing strain family in Russia. Jama. 2005;293(22):2726-31.
16. van Crevel R, Nelwan RH, de Lenne W, Veeraragu Y, van der Zanden AG, Amin Z, et al. Mycobacterium tuberculosis Beijing genotype strains associated with febrile response to treatment. Emerg Infect Dis. 2001;7(5):880-3.

17. Ordway D, Henao-Tamayo M, Harton M, Palanisamy G, Troudt J, Shanley C, et al. The hypervirulent Mycobacterium tuberculosis strain HN878 induces a potent TH1 response followed by rapid down-regulation. J Immunol. 2007;179(1):522-31.
18. de Steenwinkel JE, ten Kate MT, de Knegt GJ, Verbrugh HA, Aarnoutse RE, Boeree MJ, et al. Consequences of noncompliance for therapy efficacy and emergence of resistance in murine tuberculosis caused by the Beijing genotype of Mycobacterium tuberculosis. Antimicrob Agents Chemother. 2012;56(9):4937-44.
19. Manca C, Tsenova L, Bergtold A, Freeman S, Tovey M, Musser JM, et al. Virulence of a Mycobacterium tuberculosis clinical isolate in mice is determined by failure to induce Th1 type immunity and is associated with induction of IFN-alpha /beta. Proc Natl Acad Sci U S A. 2001;98(10):5752-7.
20. Manca C, Tsenova L, Freeman S, Barczak AK, Tovey M, Murray PJ, et al. Hypervirulent M. tuberculosis W/Beijing strains upregulate type I IFNs and increase expression of negative regulators of the Jak-Stat pathway. J Interferon Cytokine Res. 2005;25(11):694-701.
21. Reed MB, Domenech P, Manca C, Su H, Barczak AK, Kreiswirth BN, et al. A glycolipid of hypervirulent tuberculosis strains that inhibits the innate immune response. Nature. 2004;431(7004):84-7.
22. Tsenova L, Ellison E, Harbacheuski R, Moreira AL, Kurepina N, Reed MB, et al. Virulence of selected Mycobacterium tuberculosis clinical isolates in the rabbit model of meningitis is dependent on phenolic glycolipid produced by the bacilli. J Infect Dis. 2005;192(1):98-106.
23. Shang S, Harton M, Tamayo MH, Shanley C, Palanisamy GS, Caraway M, et al. Increased Foxp3 expression in guinea pigs infected with W-Beijing strains of M. tuberculosis. Tuberculosis (Edinb). 2011;91(5):378-85.
24. Aguilar D, Hanekom M, Mata D, Gey van Pittius NC, van Helden PD, Warren RM, et al. Mycobacterium tuberculosis strains with the Beijing genotype demonstrate variability in virulence associated with transmission. Tuberculosis (Edinb). 2010;90(5):319-25.
25. Mourik BC, de Knegt GJ, Verbon A, Mouton JW, Bax HI, de Steenwinkel JEM. Assessment of Bactericidal Drug Activity and Treatment Outcome in a Mouse Tuberculosis Model Using a Clinical Beijing Strain. Antimicrob Agents Chemother. 2017;61(10).
26. De Steenwinkel JE, De Knegt GJ, Ten Kate MT, Van Belkum A, Verbrugh HA, Hernandez-Pando R, et al. Immunological parameters to define infection progression and therapy response in a well-defined tuberculosis model in mice. Int J Immunopathol Pharmacol. 2009;22(3):723-34.
27. de Steenwinkel JE, ten Kate MT, de Knegt GJ, Kremer K, Aarnoutse RE, Boeree MJ, et al. Drug susceptibility of Mycobacterium tuberculosis Beijing genotype and association with MDR TB. Emerg Infect Dis. 2012;18(4):660-3.
28. Krishnan N, Malaga W, Constant P, Caws M, Tran TH, Salmons J, et al. Mycobacterium tuberculosis lineage influences innate immune response and virulence and is associated with distinct cell envelope lipid profiles. PLoS One. 2011;6(9):e23870.
29. Mourik BC, Leenen PJ, de Knegt GJ, Huizinga R, van der Eerden BC, Wang J, et al. Immunotherapy Added to Antibiotic Treatment Reduces Relapse of Disease in a Mouse Model of Tuberculosis. Am J Respir Cell Mol Biol. 2017;56(2):233-41.
30. Mayer-Barber KD, Andrade BB, Barber DL, Hieny S, Feng CG, Caspar P, et al. Innate and adaptive interferons suppress IL-1alpha and IL-1beta production by distinct pulmonary myeloid subsets during Mycobacterium tuberculosis infection. Immunity. 2011;35(6):1023-34.
31. Cooper AM, Kipnis A, Turner J, Magram J, Ferrante J, Orme IM. Mice lacking bioactive IL-12 can generate protective, antigen-specific cellular responses to mycobacterial infection only if the IL-12 p40 subunit is present. J Immunol. 2002;168(3):1322-7.

32. Mishra BB, Rathinam VA, Martens GW, Martinot AJ, Kornfeld H, Fitzgerald KA, et al. Nitric oxide controls the immunopathology of tuberculosis by inhibiting NLRP3 inflammasome-dependent processing of IL-1beta. Nat Immunol. 2013;14(1):52-60.
33. Antonelli LR, Gigliotti Rothfuchs A, Goncalves R, Roffe E, Cheever AW, Bafica A, et al. Intranasal Poly-IC treatment exacerbates tuberculosis in mice through the pulmonary recruitment of a pathogen-permissive monocyte/macrophage population. J Clin Invest. 2010;120(5):1674-82.
34. Rubio D, Xu RH, Remakus S, Krouse TE, Truckenmiller ME, Thapa RJ, et al. Crosstalk between the type 1 interferon and nuclear factor kappa B pathways confers resistance to a lethal virus infection. Cell Host Microbe. 2013;13(6):701-10.
35. Greenberg SA, Higgs BW, Morehouse C, Walsh RJ, Kong SW, Brohawn P, et al. Relationship between disease activity and type 1 interferon- and other cytokine-inducible gene expression in blood in dermatomyositis and polymyositis. Genes Immun. 2012;13(3):207-13.
36. Berry MP, Graham CM, McNab FW, Xu Z, Bloch SA, Oni T, et al. An interferon-inducible neutrophil-driven blood transcriptional signature in human tuberculosis. Nature. 2010;466(7309):973-7.
37. Kozakiewicz L, Chen Y, Xu J, Wang Y, Dunussi-Joannopoulos K, Ou Q, et al. B cells regulate neutrophilia during Mycobacterium tuberculosis infection and BCG vaccination by modulating the interleukin-17 response. PLoS Pathog. 2013;9(7):e1003472.
38. Gopal R, Monin L, Slight S, Uche U, Blanchard E, Fallert Junecko BA, et al. Unexpected role for IL-17 in protective immunity against hypervirulent Mycobacterium tuberculosis HN878 infection. PLoS Pathog. 2014;10(5):e1004099.
39. Domingo-Gonzalez R, Das S, Griffiths KL, Ahmed M, Bambouskova M, Gopal R, et al. Interleukin-17 limits hypoxia-inducible factor 1alpha and development of hypoxic granulomas during tuberculosis. JCI Insight. 2017;2(19).
40. Phuah J, Wong EA, Gideon HP, Maiello P, Coleman MT, Hendricks MR, et al. Effects of B Cell Depletion on Early Mycobacterium tuberculosis Infection in Cynomolgus Macaques. Infect Immun. 2016;84(5):1301-11.
41. Mourik BC, Lubberts E, de Steenwinkel JEM, Ottenhoff THM, Leenen PJM. Interactions between Type 1 Interferons and the Th17 Response in Tuberculosis: Lessons Learned from Autoimmune Diseases. Front Immunol. 2017;8:294.
42. Lu LL, Chung AW, Rosebrock TR, Ghebremichael M, Yu WH, Grace PS, et al. A Functional Role for Antibodies in Tuberculosis. Cell. 2016;167(2):433-43 e14.
43. Joosten SA, van Meijgaarden KE, Del Nonno F, Baiocchini A, Petrone L, Vanini V, et al. Patients with Tuberculosis Have a Dysfunctional Circulating B-Cell Compartment, Which Normalizes following Successful Treatment. PLoS Pathog. 2016;12(6):e1005687.
44. Hernandez-Pando R, Rook GA. The role of TNF-alpha in T-cell-mediated inflammation depends on the Th1/Th2 cytokine balance. Immunology. 1994;82(4):591-5.
45. Manca C, Reed MB, Freeman S, Mathema B, Kreiswirth B, Barry CE, 3rd, et al. Differential monocyte activation underlies strain-specific Mycobacterium tuberculosis pathogenesis. Infect Immun. 2004;72(9):5511-4.
46. Khader SA, Partida-Sanchez S, Bell G, Jelley-Gibbs DM, Swain S, Pearl JE, et al. Interleukin 12p40 is required for dendritic cell migration and T cell priming after Mycobacterium tuberculosis infection. The Journal of experimental medicine. 2006;203(7):1805-15.
47. Reyes-Martinez JE, Nieto-Patlan E, Nieto-Patlan A, Gonzaga-Bernachi J, Santos-Mendoza T, Serafin-Lopez J, et al. Differential activation of dendritic cells by Mycobacterium tuberculosis Beijing genotype. Immunological investigations. 2014;43(5):436-46.

48. Koo MS, Subbian S, Kaplan G. Strain specific transcriptional response in Mycobacterium tuberculosis infected macrophages. Cell Commun Signal. 2012;10(1):2.
49. Askenase MH, Han SJ, Byrd AL, Morais da Fonseca D, Bouladoux N, Wilhelm C, et al. Bone-Marrow-Resident NK Cells Prime Monocytes for Regulatory Function during Infection. Immunity. 2015;42(6):1130-42.